

Confinement studies in the TJ-II stellarator

C Alejaldre†, J Alonso†, L Almoguera†, E Ascasíbar†, A Baciero†,
 R Balbín†, M Blaumoser†, J Botija†, B Brañas†, E de la Cal†, A Cappa†,
 R Carrasco†, F Castejón†, J R Cepero†, C Cremy†, J M Delgado†, J Doncel†,
 C Dulya†, T Estrada†, A Fernández†, C Fuentes†, A García†,
 I García-Cortés†, J Guasp, J Herranz†, C Hidalgo†, J A Jiménez†,
 I Kirpichev†, V Krivenski†, I Labrador†, F Lapayese†, K Likin†, M Linier†,
 A López-Fraguas†, A López-Sánchez†, E de la Luna†, R Martín†,
 A Martínez†, L Martínez-Laso†, M Medrano†, P Méndez†, K J McCarthy†,
 F Medina†, B van Milligen†, M Ochando†, L Pacios†, I Pastor†,
 M A Pedrosa†, A de la Peña†, A Portas†, J Qin†, L Rodríguez-Rodrigo†,
 A Salas†, E Sánchez†, J Sánchez†, F Tabarés†, D Tafalla†, V Tribaldos†,
 J Vega†, B Zurro†, D Akulina‡, O I Fedyanin‡, S Grebenschikov‡,
 N Kharchev‡, A Meshcheryakov‡, K A Sarkisian‡, R Barth§, G van Dijk§ and
 H van der Meiden§

† Asociación Euratom-Ciemat, 28040 Madrid, Spain

‡ General Physics Institute, Moscow, Russia

§ FOM-Instituut voor Plasmafysica 'Rijnhuizen', The Netherlands

Received 18 June 1999

Abstract. ECR (electron cyclotron resonance) heated plasmas have been studied in the low magnetic shear TJ-II stellarator ($R = 1.5$ m, $a < 0.22$ m, $B = 1$ T, $f = 53.2$ GHz, $P_{\text{ECRH}} = 300$ kW, power density = $1\text{--}25$ W cm $^{-3}$). Recent experiments have explored the flexibility of the TJ-II across a wide range of plasma volumes with different rotational transforms and rational surface densities. In this paper, the main results of this campaign are presented and, in particular, the influence of iota and rational surfaces on plasma profiles is discussed.

1. Introduction

The TJ-II is a low magnetic shear stellarator of the Helic type with an average major radius of 1.5 m and an average minor radius, $a \leq 0.22$ m [1]. The magnetic field ($B_0 \leq 1.2$ T) is generated by a system of poloidal, toroidal and vertical field coils. The central conductors, which provide the flexibility of the TJ-II device, consist of a circular coil and two helical coils wrapped around the central conductor. The main characteristics of the TJ-II are (a) the strong helical variation of its magnetic axis, (b) very favourable MHD (magnetohydrodynamics) characteristics with the potential for high-beta operation and (c) bean-shaped plasmas with a wide range of operational flexibility (i.e. its rotational transform and magnetic well depth can be varied over a wide range). Two gyrotrons (53.2 GHz, up to 700 kW total) have been installed for the first stage. In the second stage, 2 MW of additional NBI (neutral beam injection) will be available. In addition, a state-of-the-art set of plasma diagnostics has been installed. Furthermore, a powerful data acquisition system is in operation to handle

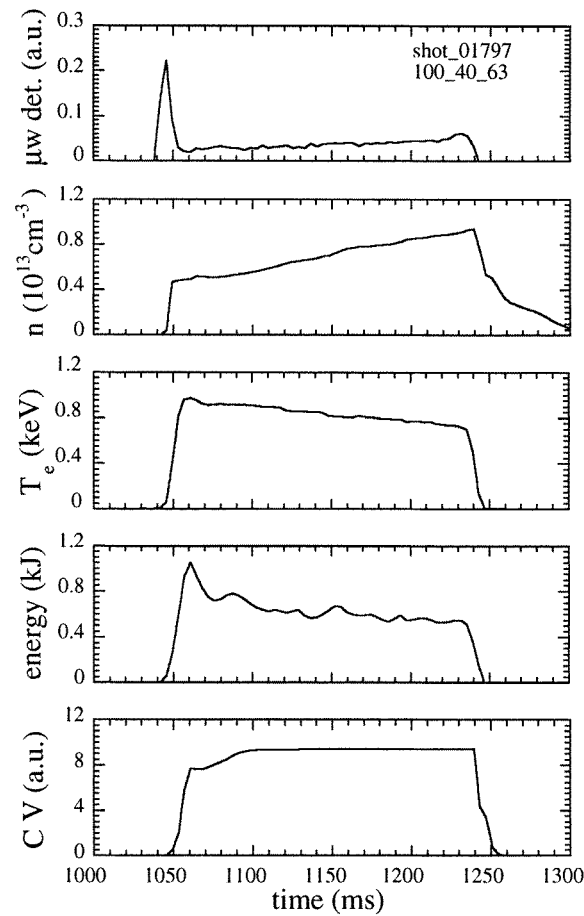


Figure 1. Time evolution of plasma parameters. From top to bottom: ECR microwave detector, line averaged density, central electron temperature (ECE), diamagnetic stored energy and C v impurity line.

the large amounts of data (≈ 125 Mbyte/discharge). The physics programme of the TJ-II stellarator is focused on transport studies in low-collisionality plasmas, operational limits in high-beta plasmas, and on studies of transport optimization and its relation to the radial electric field.

1.1. Characteristics of the ECRH system

The ECRH (electron cyclotron resonance heating) system consists of two 350 kW gyrotrons ($f = 53.2$ GHz) with a pulse length up to 1 s. The gyrotrons are coupled to the plasma by means of two quasi-optical transmission lines. The first quasi-optical transmission line (QTL1) allows perpendicular power injection, while the second one (QTL2) is equipped with a movable mirror, located inside the vacuum chamber, that can be rotated both poloidally and toroidally. This movable mirror allows the power deposition position to be varied, while also inducing current by electron cyclotron current drive (ECCD). The power density at resonances ranges from 1 W cm^{-3} for the QTL1 line to 25 W cm^{-3} for the QTL2 line. A power transmission efficiency of 0.9 has been achieved along the

mirror lines and the wave beam diameter is ~ 10 cm (QTL1) and ~ 2 cm (QTL2) at the plasma border. Measurements show that the residual microwave power not absorbed directly by the plasma bulk is absorbed after a few passes through the plasma column. This is in agreement with the extensive linear ray-tracing calculations carried out to analyse the performance of the ECRH system in the TJ-II. The first plasmas were achieved with the QTL1 line [1], whereas the results presented in this paper were obtained with the QTL2 line.

1.2. Wall conditioning

The main improvement made in wall conditioning of the TJ-II vacuum vessel with respect to the previous campaign [1] has been its baking at 150°C . A factor of five decrease in the total pressure was obtained at room temperature after cooling, and this was consistent with the decrease in the water peak in the residual gas analyser (RGA). Base pressures in the range of 5×10^{-8} mbar were systematically achieved afterwards, even after the vacuum vessel had been pressurized for diagnostic or heating-system maintenance. The better vacuum conditions had two direct consequences on machine operation. Firstly, a dramatic reduction was observed in x-ray generation during current ramp-up and microwave heating. Secondly, strong focusing of the microwave beam (QTL2) onto the groove area close to the plasma axis was fully compatible with plasma generation and heating, even when the localized temperature increased. This localized temperature increase, due to weak absorption of the RF beam on the stainless-steel surface, was determined to be $\approx 100^\circ\text{C}$ from the increase in the water desorption rate observed during the heating pulse.

1.3. Edge topology

The plasma is naturally limited by part of the vacuum vessel, acting as a helical belt limiter or, alternatively, by two mobile poloidal limiters. The geometry of the TJ-II vacuum chamber and flux surfaces makes the magnetic connection length in the SOL (scrape-off layer) strongly dependent on the radial distance to the last closed magnetic surface (LCMS). Field mapping calculations have shown that the characteristic connection length for field lines outside the last closed flux surface (LCFS) that interact with the vacuum chamber is in the range 2–15 m. This value increases to 20–200 m for field lines interrupted only by the mobile limiters. In agreement with these calculations, the e-folding length of plasma edge profiles increases from about 1 cm with the helical limiter to about 2 cm for the poloidal limiter configuration. A reduction in plasma fuelling by wall impurities is observed as the poloidal limiter is inserted into the plasma [2]. In the experiments reported in this paper, the plasma was limited by the vacuum chamber (helical belt limiter).

2. Plasma profiles and transport in ECRH plasmas

The time evolution of a ECRH discharge is shown in figure 1. Plasma discharges lasting up to 300 ms with central electron temperatures up to 1 keV, plasma densities in the range $(0.5\text{--}1.5) \times 10^{19} \text{ m}^{-3}$, and global energy confinement times up to 4 ms have been achieved using 250 kW of heating power (P_{ECRH}) with a power density of 25 W cm^{-3} . Confinement properties have been found to be strongly dependent on plasma configuration.

A systematic delay of 3–4 ms was obtained between ECRH injection and plasma breakdown. However a longer delay of up to tens of milliseconds was observed before the onset of plasma heating. This delay was seen to be a strong function of the neutral pressure present in

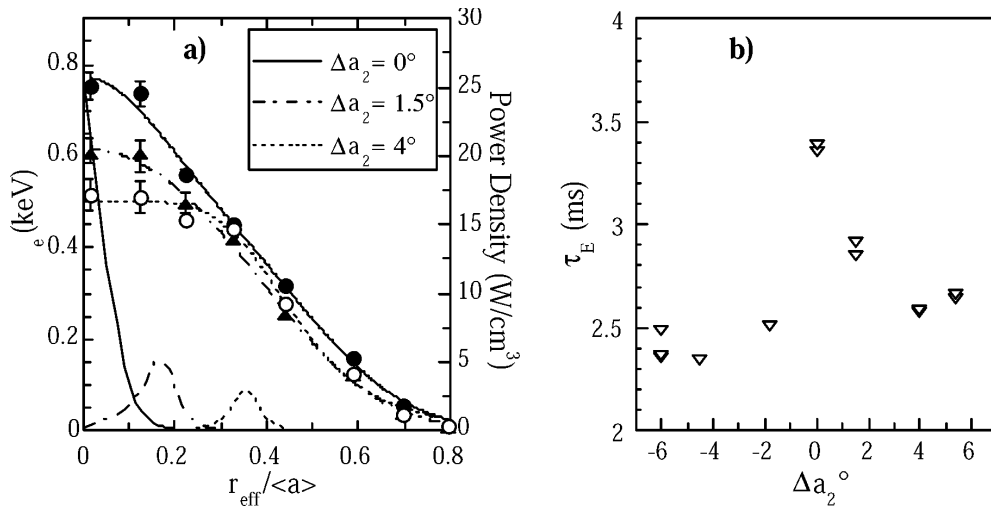


Figure 2. (a) Electron temperature and ECRH deposition profiles from linear ray-tracing calculations, and (b) energy confinement time versus poloidal angle of the internal mirror.

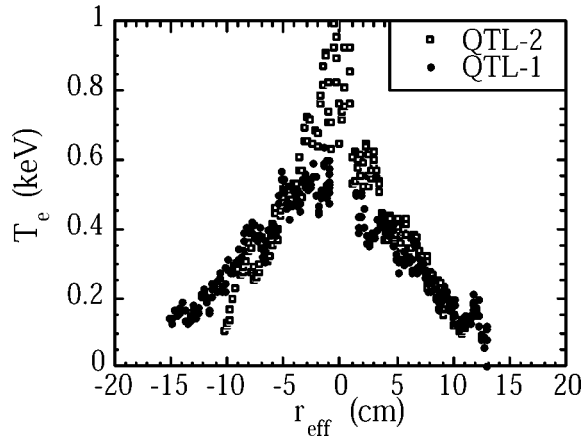


Figure 3. Electron temperatures in ECRH plasmas with different ECRH power densities.

the vessel at the time of RF launching. A simple parametric analysis suggests the presence of a critical, maximum neutral pressure for plasma heating to take place, the delay being closely related to the time required for the decay of the initial molecular density to reach such a threshold value. This behaviour significantly differs from that observed in the previous campaign, where a much lower power density was available for plasma initiation, and it is presently being investigated.

ECRH deposition profiles have an effect on temperature profiles and confinement times for different poloidal angles of the internal mirror of the QTL2 line. Thomson scattering and ECE (electron cyclotron emission) system measurements show peaked temperature profiles but rather flat density profiles in on-axis ECR heated discharges, while in off-axis heated discharges the central electron temperature and the energy confinement time decrease (see figure 2). In this experiment, the x-ray flux (20–200 keV) decreases as the confinement time decreases. Non-Maxwellian features have been observed in electron distribution functions

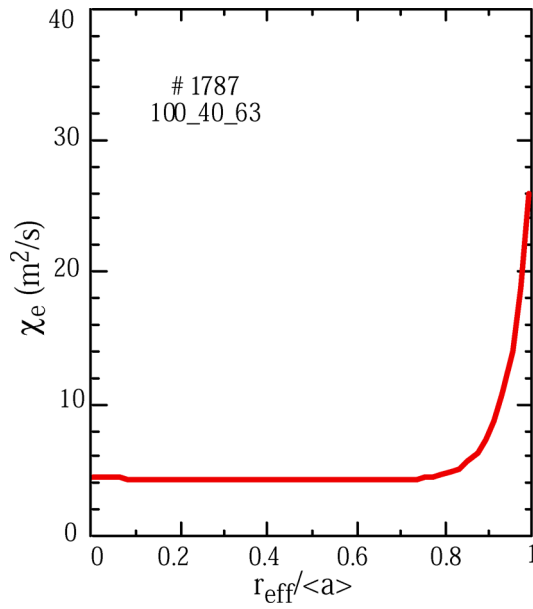


Figure 4. Radial profile of electron heat conductivity deduced from the transport code proctor for a configuration with $\iota(a) \approx 1.6$.

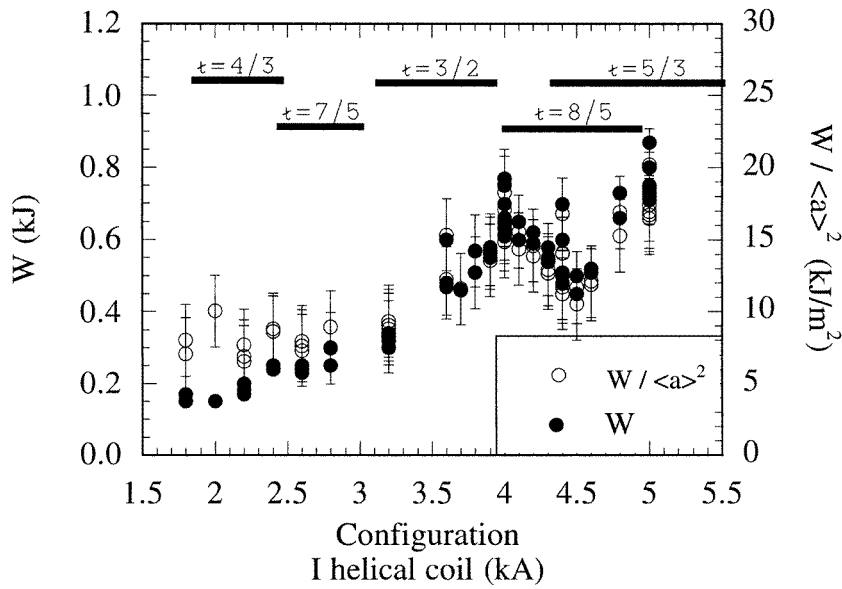


Figure 5. Energy content as a function of the magnetic configuration. Full symbols (W): diamagnetic stored energy averaged along the discharge. Open symbols ($W a^{-2}$): previous values normalized to the plasma volume of each corresponding configuration. Error bars are shown only in the normalized energy values for the sake of clarity. The thick horizontal bars in the upper part of the box show the calculated configuration range along which the major low-order rational iota values are inside the plasma.

over the 1–5 keV energy range. Their possible link with ECRH-induced deformation of the electron distribution is under investigation [3].

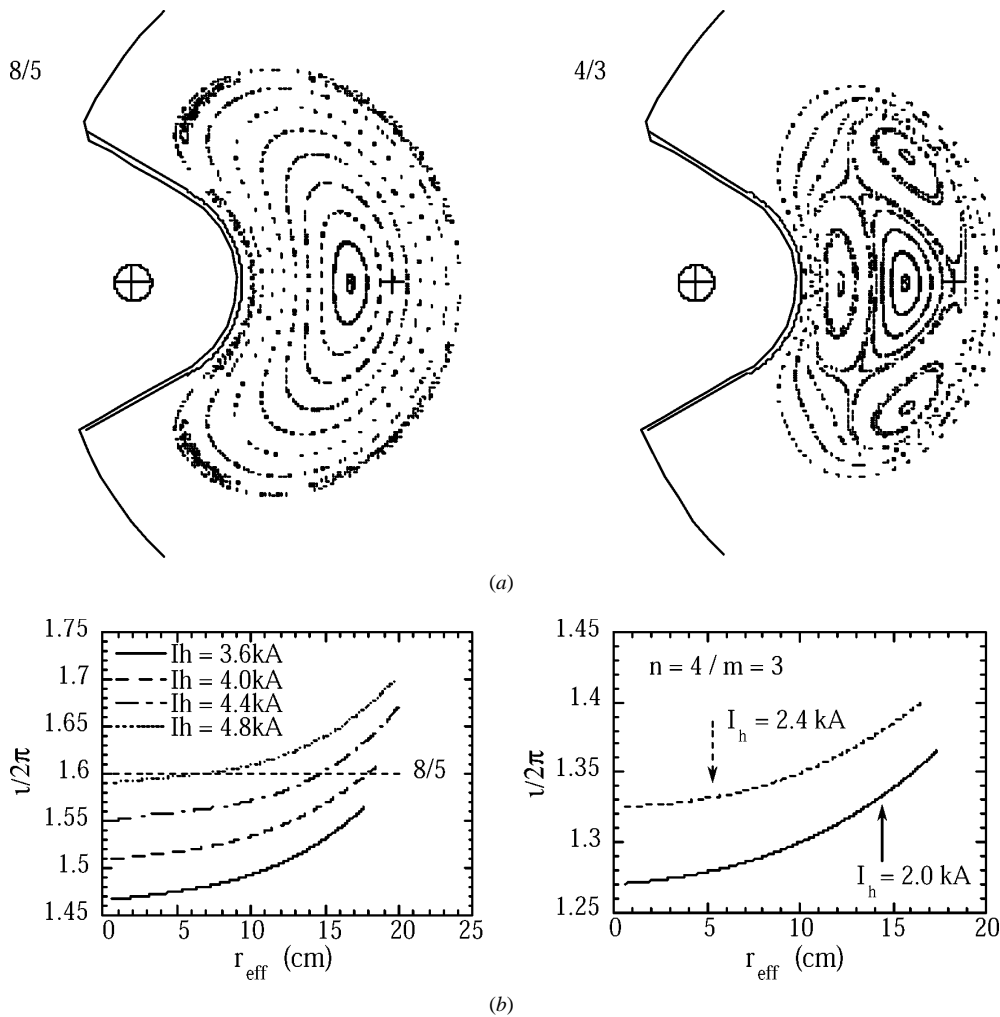


Figure 6. TJ-II vacuum configurations showing the 4/3 and 8/5 resonances. (a) Magnetic field structure. (b) Iota profile dependence on I_{hx} .

The ECRH power density has an influence on the maximum central electron temperatures attainable. This effect is seen in figure 3, where electron temperature profiles in ECRH plasmas with power densities of 1 W cm^{-3} (QTL1 line) and 25 W cm^{-3} (QTL2 line) are compared.

The predictive transport code Proctor has been used for a preliminary investigation of transport in ECRH plasmas [4]. In the ECRH discharges studied, where plasma densities were less than $1.7 \times 10^{19} \text{ m}^{-3}$, and where the collisional electron-ion coupling and the total radiative power were rather small ($<40\%$), the electron heat conduction is expected to be the dominant loss channel. In the present simulation, the electron heat conductivity is assumed to depend on electron density and temperature as in the LHD (Large Helical Device) scaling law. Figure 4 shows the simulated electron conductivity profile. The heat conductivity is about $4 \text{ m}^2 \text{ s}^{-1}$ in the plasma core region and increases as the plasma boundary region is approached. Monte Carlo computations of neo-classical transport in the TJ-II stellarator have also been made, and show that the expected neo-classical energy confinement time is about a factor of two larger than that measured experimentally [5]. For typical TJ-II plasma conditions, i.e., the long mean

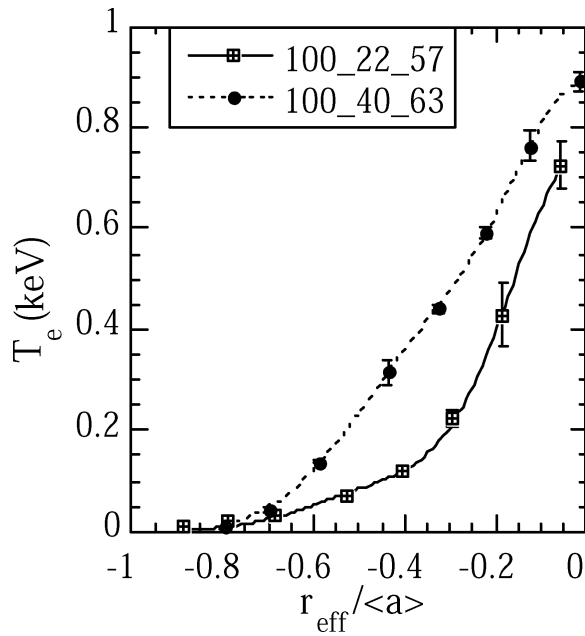


Figure 7. Plasma profiles with and without 4/3 resonance inside the plasma as predicted by field line vacuum calculations.

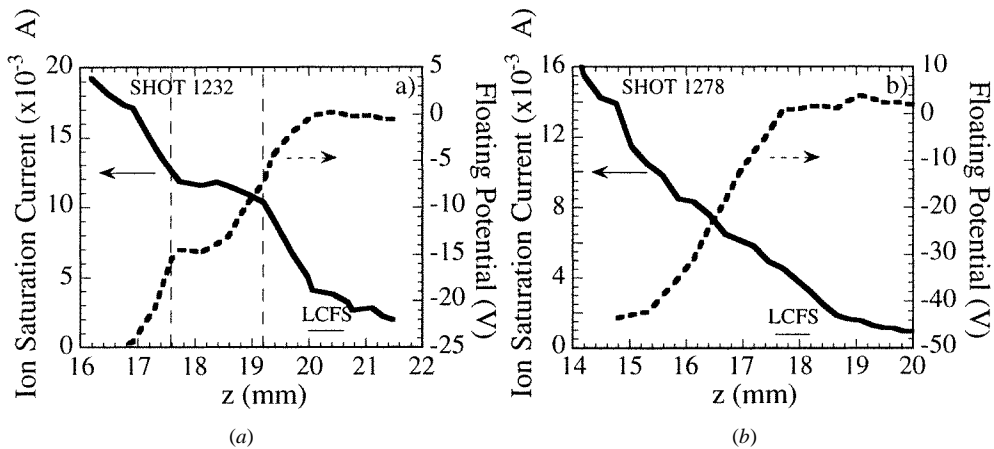


Figure 8. Ion saturation current and floating potential profiles for plasma configurations with (a) $\iota/2\pi \approx 1.6$, and (b) $\iota/2\pi \approx 1.5$.

free path collisionality regime, the ambipolar radial electric field is expected to be positive. This is in agreement with poloidal rotation measurements made in the TJ-II, which show that impurity ions (as determined from C ν lines) rotate in the ion-diamagnetic drift direction and it is consistent with positive radial electric fields in the range of tens of volts per centimetre [6, 7].

3. Configuration effects: rotational transform and rational surfaces

The investigation of the influence of plasma resonances and iota on plasma profiles and confinement is in progress in the TJ-II stellarator. The magnetic field is generated in the

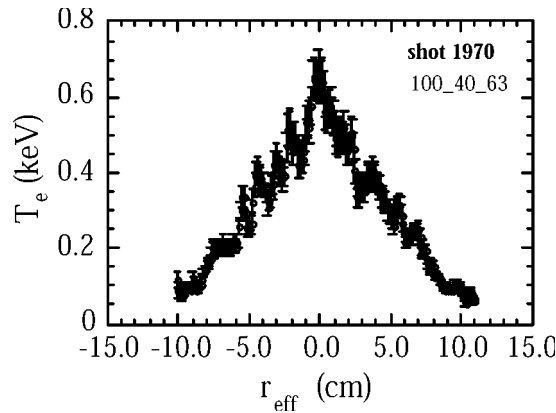


Figure 9. Temperature profile measured with a high-resolution Thomson system.

TJ-II by a system of poloidal, toroidal, vertical and central coils. The central conductors, consisting of a circular coil (I_{cc}) and two helical coils (I_{hx}), provide the flexibility of the TJ-II device. The radial location of rational surfaces can be varied over a wide range of rotational transform values by changing the I_{cc} and I_{hx} currents.

Global confinement properties have been found to be strongly dependent on plasma configuration. Figure 5 shows the stored energy for a plasma configuration scan ($I_{hx} = 1.8\text{--}5.0$ kA, $I_{cc} = 10$ kA). In this scan, both the plasma volume ($0.52\text{--}1.10$ m³) and the rotational transform ($iota(a) = 1.32\text{--}1.73$) were modified. The optimal confinement has been found for $I_{hx} \approx 4.0$ kA when major low-order resonances are avoided. Interestingly, $W a^{-2}$ increases with I_{hx} (i.e. $iota$), thus suggesting improved stored energy with $iota$.

A magnetic configuration scan was performed to move the $4/3$ and $8/5$ natural resonances from the edge to the central region of the plasma (figure 6). Because TJ-II has low magnetic shear, the low-order $4/3$ resonance has a considerable effect on global confinement and plasma profiles. Figure 7 shows the comparison between electron temperature profiles measured in plasma configurations with and without the $4/3$ resonance inside the plasma, as predicted by field line vacuum calculations. It is seen here that plasma profiles are significantly modified.

The presence of the natural $8/5$ rational surface in the plasma boundary region, as predicted by equilibrium codes for this configuration, has been detected as a flattening in edge profiles (see figure 8). However, the flattening (with a radial extension of about 1 cm) in density and potential profiles is not the same. The experiments performed indicate the formation of $\mathbf{E} \times \mathbf{B}$ sheared flows in the proximity of rational surfaces ($8/5$) in the TJ-II stellarator. The resulting shearing rate is comparable to the inverse of the fluctuation correlation time [8]. Different mechanisms should be considered for the generation of $\mathbf{E} \times \mathbf{B}$ flows at resonant surfaces. For instance, $\mathbf{E} \times \mathbf{B}$ flows can be driven by the ion–electron flux difference created in the vicinity of rational surfaces. The $\mathbf{E} \times \mathbf{B}$ sheared flows linked to the radial location of rational surfaces could also be explained by taking into account the rational surface-induced anisotropy in the structure of turbulence [9]. Radially varying non-isotropic turbulence allows fluctuations to rearrange the profile of poloidal momentum, thereby generating sheared poloidal flows. Sheared $\mathbf{E} \times \mathbf{B}$ flows linked to resonant surfaces could explain the spontaneous formation of transport barriers at rational surfaces in fusion plasmas and open a research area to induce internal transport barriers in fusion plasmas.

High-spatial-resolution, Thomson scattering measurements [10] have revealed the presence of a fine structure in both density and temperature profiles (see figure 9). Their

possible link to the iota profile (i.e. rational surfaces) and the influence of plasma parameters (collisionality, magnetic well) is being investigated at present.

4. Conclusions

Plasma discharges, using a new transmission line with a power density in the order of 25 W cm^{-3} ($P_{\text{ECRH}} = 300 \text{ kW}$), with central temperatures up to 1 keV and energy confinement time up to 4 ms have been achieved. Temperature profiles react to ECR on/off-axis heating.

Configuration scan studies show a significant modification in plasma profiles and stored energies in the TJ-II. Stored energy scales with iota and plasma volume, while high-resolution, Thomson scattering profiles show fine structures.

Evidence of sheared $\mathbf{E} \times \mathbf{B}$ flows associated with the presence of rational surfaces has been observed in the edge region of the TJ-II stellarator. This mechanism may explain the spontaneous formation of transport barriers at rational surfaces in magnetically confined plasmas.

Acknowledgments

This research was sponsored in part by DGICYT (Dirección General de Investigaciones Científicas y Técnicas) of Spain under project PB96-0112-C2-02 and PB97-0160.

References

- [1] Alejandre C *et al* 1999 *Plasma Phys. Control. Fusion* **41** A539–48
- [2] Tabarés F L *et al* 1999 *Plasma Phys. Control. Fusion, Proc. 26th EPS Conf. on Controlled Fusion and Plasma Physics* ed B Schweer, G Van Oost and E Vietzke, vol 23J, p 369
- [3] Rodríguez-Rodrigo L, Medina F, Ochando M A and López-Fraguas A 1999 *Plasma Phys. Control. Fusion, Proc. 26th EPS Conf. on Controlled Fusion and Plasma Physics* ed B Schweer, G Van Oost and E Vietzke, vol 23J, p 353
- [4] Castejón F *et al* 1999 *Plasma Phys. Control. Fusion, Proc. 26th EPS Conf. on Controlled Fusion and Plasma Physics* ed B Schweer, G Van Oost and E Vietzke, vol 23J, p 365
- [5] Tribaldos V, Guasp J and Castejón F 1999 *Plasma Phys. Control. Fusion, Proc. 26th EPS Conf. on Controlled Fusion and Plasma Physics* ed B Schweer, G Van Oost and E Vietzke, vol 23J, p 349
- [6] Zurro B *et al* 1999 *Plasma Phys. Control. Fusion, Proc. 26th EPS Conf. on Controlled Fusion and Plasma Physics* ed B Schweer, G Van Oost and E Vietzke, vol 23J, p 357
- [7] McCarthy K J, Zurro B, Baciero A and Cremy C 1999 *Plasma Phys. Control. Fusion, Proc. 26th EPS Conf. on Controlled Fusion and Plasma Physics* ed B Schweer, G Van Oost and E Vietzke, vol 23J, p 389
- [8] Pedrosa M A *et al* 1999 *Plasma Phys. Control. Fusion, Proc. 26th EPS Conf. on Controlled Fusion and Plasma Physics* ed B Schweer, G Van Oost and E Vietzke, vol 23J, p 377
- [9] Hidalgo C *et al* 1999 *Phys. Rev. Lett.* **83** 2203
- [10] Barth C J *et al* 1999 *Rev. Sci. Instrum.* **70** 1 763–7

